Since January 2020 Elsevier has created a COVID-19 resource centre with free information in English and Mandarin on the novel coronavirus COVID-19. The COVID-19 resource centre is hosted on Elsevier Connect, the company's public news and information website.

Immunology Letters 129 (2010) 13–22

Contents lists available at ScienceDirect

Immunology Letters

journal homepage: www.elsevier.com/locate/

Structure–function analysis and molecular modeling of DNase catalytic antibodies

Haggag S. Zein[a,c,*], Jaime A. Teixeira da Silva[b], Kazutaka Miyatake[c]

[a] Department of Genetics, Faculty of Agriculture, Cairo University, 12 Gamma Street, Giza 12613, Egypt
[b] Faculty of Agriculture and Graduate School of Agriculture, Kagawa University, Miki-cho, Ikenobe 2393, Kagawa-ken 761-0795, Japan
[c] Department of Applied Biological Chemistry, Graduate School of Agriculture and Biological Sciences, Osaka Prefecture University, 1-1, Gakuen-Cho, Sakai, Osaka 599-8531, Japan

ARTICLE INFO

Article history:
Received 24 November 2009
Received in revised form
26 December 2009
Accepted 14 January 2010
Available online 25 January 2010

Keywords:
Monoclonal antibodies
Cucumber mosaic virus
Antibody genes
DNase catalytic activities
Anti-DNA antibodies

ABSTRACT

There is great interest in the antibodies-to-DNA transformation, since this change is characteristic of autoimmune diseases and contributes to its pathology. After immunization and fusions, 14 hybridomas bearing DNA-hydrolysis activity against pUC19 plasmid DNA were obtained. Genes coding for V_H and V_L regions of the 14 monoclonal antibodies (mAbs) were cloned and sequenced. The sequences were compared with sequences of the Ig-Blast database to determine their germline and to identify potential mutations responsible for DNA binding and DNase activity. V genes of the H chains' genes expressed four genes of the V_H1/J558 family, three of V_H5/V_H7183, and three of V_H8/V_H3609. The genetic repertoire of these mAbs was examined by determining the nucleotide sequences of their H chain V regions. This V_H and V_L domain was most similar to an anti-ssDNA (DNA-1) antibody as well as to catalytic autoimmune mAb (m3D8). Computer-generated models of the three-dimensional structures of V_H and V_L (VHL4) of the IgG4 combinations were used to define the positions occupied by the important sequence motifs at the binding sites. The modeling structure showed that VHL4 binds to oligo (dT3) primarily by sandwiching thymine bases between Tyr L32, Tyr L49 and Tyr H97 side-chains. Superposing VHL4 with anti-nucleic acid m3D8 catAbs revealed a common ssDNA recognition module consisting of His L93, His H35 residues which are critical for DNA-hydrolyzing antibodies. This study demonstrates the potential usefulness of the protein DNA surrogate in the investigation of the origin of anti-DNA antibodies' hydrolyzing activities.

1. Introduction

Catalytic antibodies (catAbs) were first obtained in 1986 [1,2] against transition state analogs. Amidase and peptidase activities were found in IgGs from the sera of patients with rheumatoid arthritis [3], factor VIII-cleaving allo-Abs in the sera of patients with severe hemophilia [4], and DNA-hydrolyzing, amidolytic and peptidolytic activities in Bence–Jones proteins from patients with multiple myeloma [5]. The multiple myeloma patients of an Ab light chain that cleaves the human immunodeficiency virus protein gp120 demonstrated that natural Abs are not restricted to autoantigenic substrates [6]. Anti-DNA antibodies play an important role in the pathogenesis of systemic lupus erythematosus (SLE) in humans [7]. It has been reported that some of the catAbs to DNA found in SLE patients have nuclease activity and catalyze hydrolysis of the DNA phosphodiester bond [7]. A natural catAbs was prepared by the immunization of mice with ground-state polypeptides or proteins such as Ab light chain-specific vasoactive intestinal peptide which has peptidase hydrolytic activity [8]. Also immunizing mice by human immunodeficiency virus (HIV)-1 gp41 polypeptide-stimulated Ab light chain enzymatically cleaved the conserved region of the HIV-1 envelope protein as well as the antigenic gp41 peptide [9]. Sequence analysis of anti-DNA mAbs from both patients with SLE and murine models of the disease showed that these high-affinity anti-dsDNA IgG contain a high proportion of somatic mutations in their V_H and V_L sequences [10,11]. In many of these high-affinity anti-dsDNA IgG Abs, such somatic mutations lead to higher frequencies of certain amino acids, particularly arginine, asparagine, lysine, and tyrosine in the complementarity-determining regions (CDRs). It has been suggested that the structures of these amino acids allow them to form electrostatic interactions and hydrogen bonds with the negatively charged DNA phosphodiester backbone [11]. The aim of this work

Abbreviations: ELISA, enzyme-linked immunosorbent assay; FR, framework region; HRP, horseradish peroxidase; mAb, monoclonal antibody; PBS, phosphate-buffered saline; scFv, single chain Fv; V_H, variable heavy chain; V_L, variable light chain.

* Corresponding author. Tel.: +20 187676770/235685148; fax: +20 235717355/235720739.
E-mail addresses: haggagsalah@gmail.com, hagzein8@yahoo.com (H.S. Zein).

0165-2478/$ – see front matter © 2010 Elsevier B.V. All rights reserved.
doi:10.1016/j.imlet.2010.01.004

was to study mAbs and their DNA-hydrolyzing activities. The reactivity of the mAbs, to hydrolyse DNA, was intriguing enough to prompt us to further study their fine specificity and their catalytic mechanisms by analyzing the molecular sequence and structure of the V_H and V_L genes. Molecular modeling for stimulation with DNA catAb (m3D8) for predicting the catalytic mechanism of the variable region of mAb-4 (4 FV) and knowledge of the specific immunoglobulin genes used to target a common epitope may potentially be useful to identify protein DNA mimicry in the investigation of the origin of anti-DNA Abs catalytic activities.

2. Materials and methods

2.1. Plant material and virus purification

Tobacco plants (*Nicotiana tabacum* cv. 'Xanthi-nc') and *Nicotiana benthamiana* plants at the five-leaf stage were used for inoculation. CMV was originally obtained from *Cucurbita pepo* in Japan; CMV propagated in tobacco was purified as described by Nitta et al. [12].

2.2. Immunization

Immunized 8-week-old BALB/c mice (Nippon SLC Co., Japan) were injected subcutaneously with 100 μg of purified CMV (whole virus: coat protein contains RNAs) strain pepo in 0.1 ml phosphate-buffered saline (PBS; 0.01 M phosphate and 0.015 M sodium chloride, pH 7.5), which was mixed with an equal volume of adjuvant (RIBI; ImmunoChem Research, Inc., Hamilton, MT) and containing monophosphoryl lipid A MPL (25 μg), trehalose dicorynomycolate TDM (25 μg) and RIBI. Three injections were administered at 2-week intervals. Three days after the fourth injection, the mice were given a peritoneal injection of 200 μg of virus in 0.2 ml PBS. The mice were sacrificed 3 days later and their spleens were harvested. Fusion experiments were carried out as previously described [13]. The positive hybridoma cells were subcloned by a limiting dilution method in the presence of thymocytes of BALB/c mice as feeder cells according to standard protocols [13].

2.3. Purification of IgG

Ascites fluid (5–10 ml) was precipitated with 50% saturated ammonium sulfate, dialyzed twice for 4 h against 500 vol of (20 mM Tris–HCl, pH 8.0) at 4 °C; samples were diluted with the same amount of binding buffer (1.5 M glycine/3.0 M NaCl, pH 8.9) and the crude mAbs solution was applied to a protein A-agarose affinity chromatography column (1 ml), washed with 10 vol of binding buffer, followed by 10 vol of binding buffer containing 1% Triton X-100, and washed with 10 vol of binding buffer. The Ab was eluted (1-ml fraction) with elution buffer (0.1 M glycine, pH 2.6), and the eluant Abs were neutralized with collection buffer (1.0 M Tris, pH 9.0). The eluted mAb was dialyzed into 50 mM Tris–HCl (pH 7.5), followed by size-exclusion HPLC system chromatography on a Sephacryl-200 HR with 50 mM Tris–HCl (pH 7.5) at 4 °C according to the manufacturer's procedure.

2.4. RNA isolation and cDNA synthesis

Total RNAs were prepared from about 10^7 hybridoma cells using ISOGEN RNA extraction buffer (Nippon Gene Co., Tokyo, Japan). RNA concentration and purity were gauged using $OD_{260/280}$. The mRNAs were isolated on Oligotex-dT30 (Super) columns (Takara, Kyoto, Japan), as specified by the manufacturer's instructions. The primers used in PCR amplification were based on data by Huse et al. [14]: for V_H, 5′-AGGTCCAACTGCTCGAGTCAGG-3′ and 5′-AGGCTTACTAGTACAATCC CTGGGCACAAT-3′, where the underlined portion of the 5′ primers incorporates an XhoI site and that of the 3′ primer an SpeI restriction site. Primers for the Vκ genes were 5′-CCAGATGTGAGCTCGTGATGACCCAGACTCCA-3′ and 5′-GCGCCGTCTAGAATTAACACTCTTCCTGTTGAA-3′ where the underlined portion of the 5′ primer incorporates a SacI restriction site and that of the 3′ primer an XbaI restriction site for amplification of the Fd and κLc regions, respectively. First-strand cDNA was synthesized from mRNA template with the Moloney murine leukemia virus M-MLV Reverse Transcriptase kit (Takara, Kyoto, Japan) using oligo-dT20 primers (Pharmacia Biotech). V_H and V_L were amplified from first-strand cDNA as described by Zein et al. [15]. The amplified fragments were cloned into pGEM-T Easy Vector (1:1, 3:1, 10:1) according to the manufacturer's protocol (Promega, Biotech) and ligated with Ligation High Kit (Takara, Kyoto, Japan) for the purpose of transforming into competent *Escherichia coli* DH5α cells.

2.5. DNA sequence of V_H and V_L

Direct sequencing of the treated DNA fragments was made using M13 primer and an ABI PRISM BigDye Primer Cycle Sequencing Kit reagent following the manufacturer's instructions (Applied Biosystems) and run on an ABI Prism 310 Genetic Analyzer (Applied Biosystems) using ABI Prism Sequencing Analysis 3.7 software for data analysis. The PCR product was analyzed and sequenced using M13 primer sequencing of the V regions. Fd or Lc sequences were "blasted" against the publicly accessible "Ig-Blast" database of mouse Ig sequences at the National Center for Biotechnology Information (NCBI; http://www.ncbi.nlm.nih.gov/igblast) to determine the closest germline gene of origin, and to identify potential mutations. CDR position and numbering adopted Kabat numbering [16] and CDR definition was adopted from Andrew's web site (http://www.bioinf.org.uk/abs/).

2.6. DNA-hydrolysis assays

Assessment of catAbs' DNA-hydrolysis activities was carried out according to [15]. Briefly, an assay mixture containing 20 mM Hepes (pH 7.49), 50 mM NaCl, 1 mM $MgCl_2$, 1 mM $MnCl_2$, 2.5 μg supercoiled pUC19 plasmid DNA, and 1–5 μg of each one of the 14 mAbs clones (4, 5, 6, 7, 8, 9, 11, 52, 122, 521, M21, M22, M23, M24) prepared in 20 μl total volume was incubated for 1 h at 37 °C. Hydrolysis was assessed by 1% AGE of the reaction products; the gel was stained with ethidium bromide. Gels were photographed and scanned with Image J software. Molar ratios of reaction products were determined from the scanning data. To study the pH dependence of catalytic activity of Abs, the reactions were carried out in 50 mM acetate buffer (pH 4–5.3), 50 mM Tris–HCl (pH 7–9), carbonate buffer (pH 9.6), and 50 mM borate (pH 10) in the presence or not of 5 mM Mg^{2+}.

2.7. Structure modeling of 4-FV combining sites

3D structure models were constructed using the online Web Ab Modeling facility at the University of Bath, UK (http://www.bath.ac.uk/cpad/). Modeling is based on the AbM package using a combination of established theoretical methods together with the latest Ab structural information [16]. WAM predict was used to assign canonical classes and H-CDR3 C-terminal conformation. Structure analysis, superposition, and graphical renderings were carried out using PyMOL (Delano Scientific, San Carlos, CA). Electrostatic surface potentials were calculated using APBS [17] as a plugin (developed by Michael G. Lerner, University of Michigan) in the Pymol Molecular Graphics System (Warren L. DeLano, DeLano Scientific, San Carlos, CA, http://www.pymol.org).

Table 1
Summary of variable region gene V, (D), and J genes of the Hybridism's specific to CMV-CP.

Heavy chain[a]								Light chain				
Accession number	Clone	Isotype	V_H	Germline gene	Homology germline (%)	D gene	J_H	Accession number	Vκ	Germline gene	Homology germline (%)	Jκ
EF672206	521	1gGI	J558	J558.45	94	DSP2.11	2	EF672220	Vκ2	bd2	99	2
EF672197	4	1gGI	J558	J558.51	89	DSP2.11	2	EF672211	Vκ2	bd2	100	1
EF672202	9	1gGI	J558	J558.51	93	DSP2.11	2	EF672216	Vκ2	bd2	99	2
EF672203	11	1gGI	J558	VH104B	99	DSP2.9	2	EF672217	Vκ2	bd2	100	2
EF672198	5	1gGI	7183	7183.14	97	DSP2.7	3	EF672212	Vκ2	bd2	100	2
EF672205	52	1gGI	7183	7183.14	95	DFL16.2	4	EF672219	Vκ2	bd2	98	1
EF672201	8	1gGI	7183	68-5N	100	DSP2.7	3	EF672215	Vκ2	bd2	100	2
EF672199	6	1gGI	3609	CB17H.10	96	DFL16.1	1	EF672213	Vκ2	bd2	98	1
EF672200	7	IgG2b	3609	CB17H.10	96	DFL16.1	1	EF672214	Vκ2	bd2	99	1
EF672204	122	IgG1	3609	CB17H.10	95	DFL16.1	1	EF672218	Vκ2	bd2	100	2
EF672207	M2-1	IgG1	J558	V130.3	97	DSP2.11	2	EF672221	Vκ1A	bb1	99	4
EF672208	M2-2	IgG1	J558	V130.3	97	DSP2.11	2	EF672222	Vκ1A	bb1	100	4
EF672209	M2-3	1gGI	J558	V130.3	95	DSP2.11	2	EF672223	Vκ1A	bb1	99	4
EF672210	M2-4	1gGI	J558	V130.3	94	DSP2.11	2	EF672224	Vκ1A	bb1	100	4

[a] Closest matches from either the GenBank Databases. Germline assignments were based on the published DNA sequences.

3. Results

3.1. Production and characterization of CMV-specific mAbs

Immunization of BALB/c female mice with CMV whole virus (protein and RNAs)-stimulated Abs was intriguing: 14 mouse hybridoma cell lines secreting mAbs specific to CMV were well established. To prove that hydrolyzing activity is an intrinsic property of mAbs and is not due to copurifying enzymes, we applied some of the rigid criteria that have been previously proposed by Paul et al. [18] and regarding several aspects for high purity Abs as suggested by Nevinsky and Buneva [19]. Basically, three common steps (purification, precipitated with ammonium sulphate, and affinity chromatography) were used to remove non-specifically bound protein buffer containing 1% Triton X-100 and 0.15 M NaCl, followed by gel filtration, which resulted in Abs with a preparation purity of >99% [15].

3.2. Utilization of the V gene segments of the V_H and V_L chain genes

The V_H and Vκ regions of 14 CMV-specific mAbs generated from five different fusions of BALB/c mice were sequenced. These sequences were almost homologous with corresponding germline genes published in the GenBank database, outlined in Table 1, which summarizes the V_H, D, and J_H fragments of V_H genes, and Vκ and Jκ of V_L genes. The nucleotide and deduced amino acid sequences of the expressed light chain germline gene were confidently assigned to a very restricted germline family Vκ2, gene bd2 (10 mAbs), GenBank accession nos. (EF672211, EF672212, EF672213, EF672214, EF672215, EF672216, EF672217, EF672218, EF672219, and EF672220; Table 1). Four Abs belonged to germline family Vκ1A, gene bb1.1. GenBank accession nos. (EF672221, EF672222, EF672223, and EF672224; Table 1). The identity of the V genes used was determined by searching the GenBank database for homologies to known V genes using the BLAST protocol [20]. Alternatively, the nucleotide and deduced amino acid sequences of the expressed V_H genes of the 14 anti-CMV Abs are shown in Fig. 1 and Table 1. The V_H genes belong to the following GenBank accession nos.: V_H1/V_HJ558 (8 Abs) (EF672206, EF672197, EF672202, EF672203, EF672207, EF672208, EF672209, EF672210); V_H5/V_H7183 (3 Abs) (EF672198, EF672205, EF672201); V_H8/V_H3609 (3 Abs) (EF672199, EF672200, EF672204) (Table 1). In addition, the V_H genes of the IgG Abs were more somatically mutated. D segment usage also appears to be restricted with 7 mAbs of V_H using the DSP2 segment, while 3 mAbs were used for another segment, DFL16 (Fig. 1 and Table 2). On the other hand, it does not appear to be an obvious restriction in J_H segment usage. Interestingly, most Abs could group into three sets based on their use of the same or highly similar V_H and V_L genes [21]. Gene rearrangement entails the joining of V_H, D and J_H germline genes followed by the joining of V_L and J_L genes. The heavy chains belong to three different families classified into three subgroups. The first includes four mAbs (4, 9, 11, and 521) and belongs to the V_HJ558 germline family with different genes; the homology of the amino acid sequences are V_H104B (99%), $V_HJ558.45$ (94%), $V_HJ558.51$ (89%) and $V_HJ558.51$ (93%) [22,23] (Fig. 1E, F, G, respectively). However, the V_H genes belong to germline family V_HJ558, gene V130.3, with 97, 97, 95, and 94% identity, respectively (Fig. 1B) [24]. D segments belong to DSP2.11 combined with J_H2 (Table 1). The second subgroup includes three mAbs-(5, 8, and 52) (Fig. 1C and D) whose V_H gene segments are from the V_H7183 germline family [25]. The mAbs-(5 and 52) V_H genes are derived from the same germline gene $V_H7183.14$ with 97 and 95% amino acid homology, respectively (Fig. 1D) [26]. The third subgroup includes mAbs-(6, 7, and 122) V_H genes which are derived from the same V_H3609 germline family, CB17H.10 gene [25] with 96, 96, and 95% homology, respectively (Fig. 1A) (Table 1).

3.3. Somatic mutation and affinity maturation

Based on the sequence analyses of V genes in specific acquired immune responses to foreign antigens, somatic hypermutations were found to occur mainly in CDRs of V genes during the process of affinity maturation. The combined processes of immunoglobulin gene rearrangement and somatic hypermutation allowed for the creation of an extremely diverse Ab repertoire. V_H-521 showed 16 mutations, five of which were silent, while 11 others led to the mutation of amino acid no. 6 glutamine in germline to glutamic acid ($Gln6^HGlu$); $Ala9^HPro$; $Ser31^HLys$; $Thr54^HSer$; $Glu58^HAsp$; $Asp65^HGly$; $Ala71^HVal$; $Gln80^HGlu$; $Ser82^HHis$; $Ala94^HThr$; and $Arg95^HAsn$ (Fig. 1F). V_H-(4 and 9) showed 18 mutants, 7 silent and 11 amino acid replacements: $Thr19^HLys$; $Lys23^HArg$; $Ser25^HLue$; $Gly26^HIle$; $Met34^HVal$; $Asp52^HLue$; $Glu53^HGly$; $The54^HAsn$; and $Gly56^HAsn$; $Arg82A^HSer$; and $Lue94^HAsn$. The only difference between two V_H-(4 and 9) Abs is a one-point mutation in the V_H gene in CDRH2 $Lys65^HIle$ and another in the DSP2 segment of $Phe99^HTyr$ (Fig. 1G). In contrast, V_H-11 revealed only two substitutions, the first in CDRH2 with $Cys54^HSer$ and the second in FW3 with $Arg94^HIle$ (Fig. 1E). V_H-5 revealed 7 mutants: 2 were silent and 5 were substitutions: $Ser55^HGly$; $Tyr56^HSer$; $Arg75^HLys$; $Arg83^HLys$; $Lue89^HMet$ (Fig. 1D). V_H-52 revealed 10 mutations:

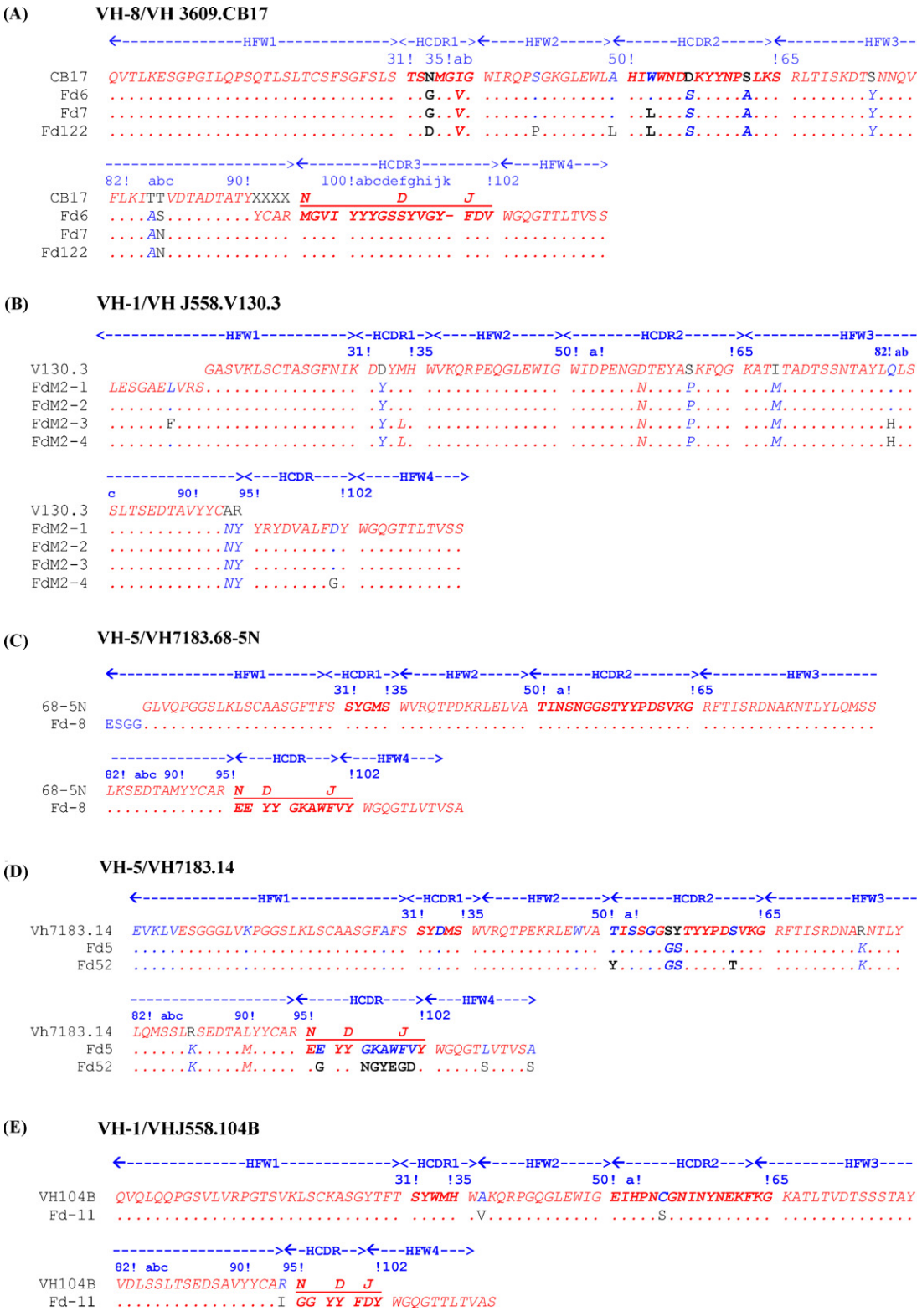

Fig. 1. Amino acid sequence alignment of the heavy chain variable regions (V_H) of the antibody-specific CMV-CP. The alignment of amino acid sequences of V_H of the CMV-specific mAbs with most closely related germline gene; V_H3609.CB17 (A); V_H J558.V130.3 (B); V_H7183.68-5N (C); V_H7183.14 (D); V_HJ558.104B (E); V_HJ558.45 (F); V_HJ558.51 (G). Germline precursors were identified as likely V_H germline candidates, respectively, through a homology search of the Kabat database. Dots represent residues identical to the corresponding germline. A dash in the individual sequences denotes a deletion. The framework region (FW) and complementarity-determining regions (CDRs) are indicated above the appropriate sequence segments in the figure. The amino acid residue is numbered according to Kabat numbering [16]. Amino acids are identified by the single-letter code.

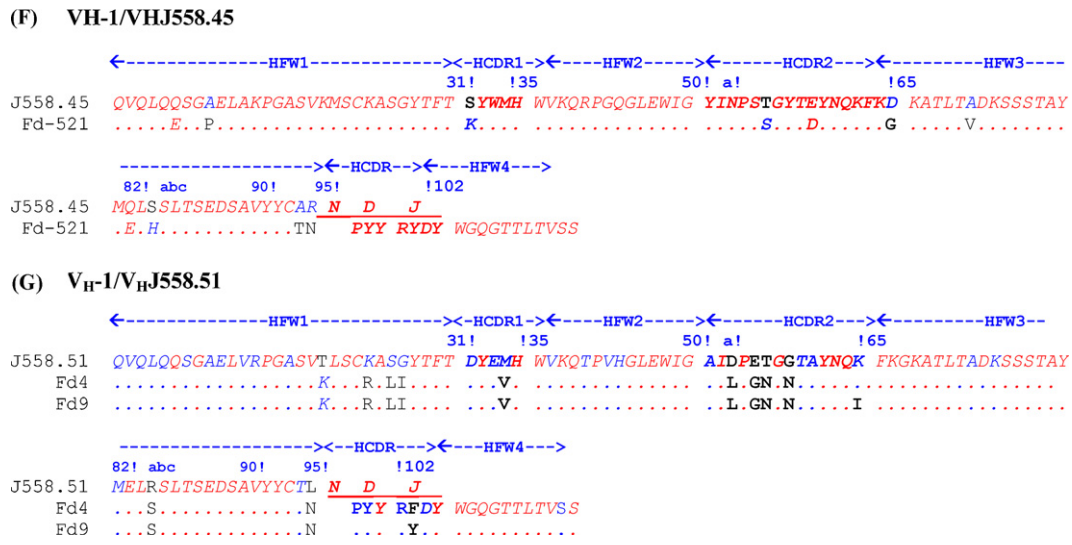

Fig. 1. (*Continued*).

3 were silent and 7 were substitutions, 5 being typical as Fd-5 with two more substitutions; Thr50^{H}Tyr and Ser62^{H}Thr (Fig. 1D). V_H-6 has 10 mutants, 3 silent and 7 substitutions: Asn33^{H}Gly; Ile35A^{H}Val; Asp56^{H}Ser; Ser62^{H}Ala; Ser74^{H}Tyr; Thr82A^{H}Ala; and Thr82B^{H}Ser. V_H-72 showed 11 mutants, 3 silent and 8 substitutions, similar to Fd-6 substitutions, except for Trp52^{H}Lue and Thr82B^{H}Asn (Fig. 1A). V_H-122 showed 13 mutants, 3 silent and 10 substitutions, similar to Fd-72, except for Asn33^{H}Asp and Ser41^{H}Pro; Ala49^{H}Lue (Fig. 1A). As the frequency of the PCR error used in this study was one in 5000–10,000 nucleotides, the intraclonal sequence heterogeneity observed here is most likely not derived from PCR errors.

3.4. CDR3 length, D regions, and number of N insertions

The length of H-CDR3 varied from 27 nucleotides in mAb-4 to 51 nucleotides in mAb-6 (Table 2). It has been suggested that the presence of Tyr and Trp residues in H-CDR3 confer flexibility upon the Ab molecule. Consequently, V_H-(6, 7, and 122) (Fig. 1A) has five Tyr residues in this region, while the other V_H has three (Table 2). There are different D and J_H regions used in the CMV-specific V_H and the number of N insertions between these regions (Table 2). On the basis of N insertions at both the V-D and the D-J_H junctions the V_H-(5, 8, and 52) (Fig. 1C and D) showed 10 nucleotides on the V_H-D side and three nucleotides on the other side, D-J_H. V_H-(5 and 8) showed 6 and 4 nucleotides on the V_H-D side, respectively, while only one nucleotide on the D-J_H side. V_H-52 showed 7 nucleotides on the V_H-D side and 5 nucleotides in the D-J_H side. V_H of the first subgroup showed only one-sided V_H-D, with 7 or 5 nucleotide insertions.

3.5. The molecular homology sequence of the V_H with GenBank database

The V_H and V_L gene families revealed high homology sequence with catAbs, and eight V_H were derived from germline gene V_HJ588. V_H-(4, 9) showed high homology sequence with different antigen-specific Abs, antinuclear Abs, hepatitis C virus neutralizing Abs [27], and anti-P24 (HIV-1) [28] (Fig. 2). In contrast, V_H8 showed sequence homology with anti-nucleic acid Abs [29] (Fig. 2), while V_H11 had high homology sequence with anti-ssDNA Ab [30] and HIV-1 capsid protein (p24)-specific Abs [31] (Fig. 2). V_H–M2-(1, 2, 3, and 4) showed high homology sequence with coronavirus-neutralizing Abs [32] (Fig. 2). Three mAbs (5, 52 and 521) are V_Hs derived from the V_H7183 family. The presumed V_H7183 germline encoding the heavy chain of this Ab has been reported in the IgM and IgG anti-DNA response in (NZB × NZW) F1 mice [33]. However, MAbs-(5 and 53) used the V_H7183.14 germline gene which showed high homology sequence with IgM polyreactive natural autoAbs [34] (Fig. 2) while mAb-8 shows high similarity with the heavy chain of influenza hemagglutinin Ha1 [35] (Fig. 2). Three mAbs (6, 7, and 122) showed high homology with anti-sweetener heavy chain [36] and similarity with mimicry of cocaine by anti-idiotypic Abs.

Table 2
Predominant CDR3 region nucleotide sequence and D segment usage of the mAbs-specific CMV.

mAbs	N	D segment	N	J_H		Length
Fd 6,7, 122	ATGGGGGTGA	TTTATTACTACGGTAGTAGCTAC	GTA	GGGTACTTCGATGTCTGGGGCGCAGGGACCACGGTCACCGTCTCCTCA	J_H1	84
Fd M21, M22, M23, M24	AA	CTACTATAGGTACGAC	GTGGCCCT	CTTTGACTACTGGGGCCAAGGCACCACTCTCACAGTCTCCTCA	J_H2	69
Fd 5	GAAGAA	TACTATGGTAA	A	GCCTGGTTTGCTTACTGGGGCCAAGGGACTCTGGTCACTGTCTCTGCA	J_H3	66
Fd 8	AGAA	TACTATGGTAA	A	GCCTGGTTTGTTTACTGGGGCCAAGGGACTCTGGTCACTGTCTCTGCA	J_H3	64
Fd 52	AGGGTTA	TTATAACGGCTACG	AGGGG	GACTACTGGGGTCAAGGAACCTCAGTCACCGTCTCCTC	J_H4	64
Fd 521	ACAAACC	CCTACTATAGGTAC		GACTACTGGGGCCAAGGCACCACTCTCACAGTCTCCTCA	J_H2	60
Fd 4	AAACC	CCTACTATAGG		TTCGACTACTGGGGCCAAGGCACCACTCTCACAGTCTCCTCA	J_H2	58
Fd 9	AAACC	CCTACTATAGG		TACGACTACTGGGGCCAAGGCACCACTCTCACAGTCTCCTCA	J_H2	58
Fd 11	ATCGG	CGGTTA		CTACTTTGACTACTGGGGCCAAGGCACCACTCTCACAGTCGCCTCA	J_H2	57

The nucleotides sequences of the different D and J_H regions that are used in the hybridomas and the number of N insertions between these regions. Comprehensive analysis of the CDR3 regions of the heavy chain. D segments in each CDR3 region and a difference in D usage, N nucleotides contribution.

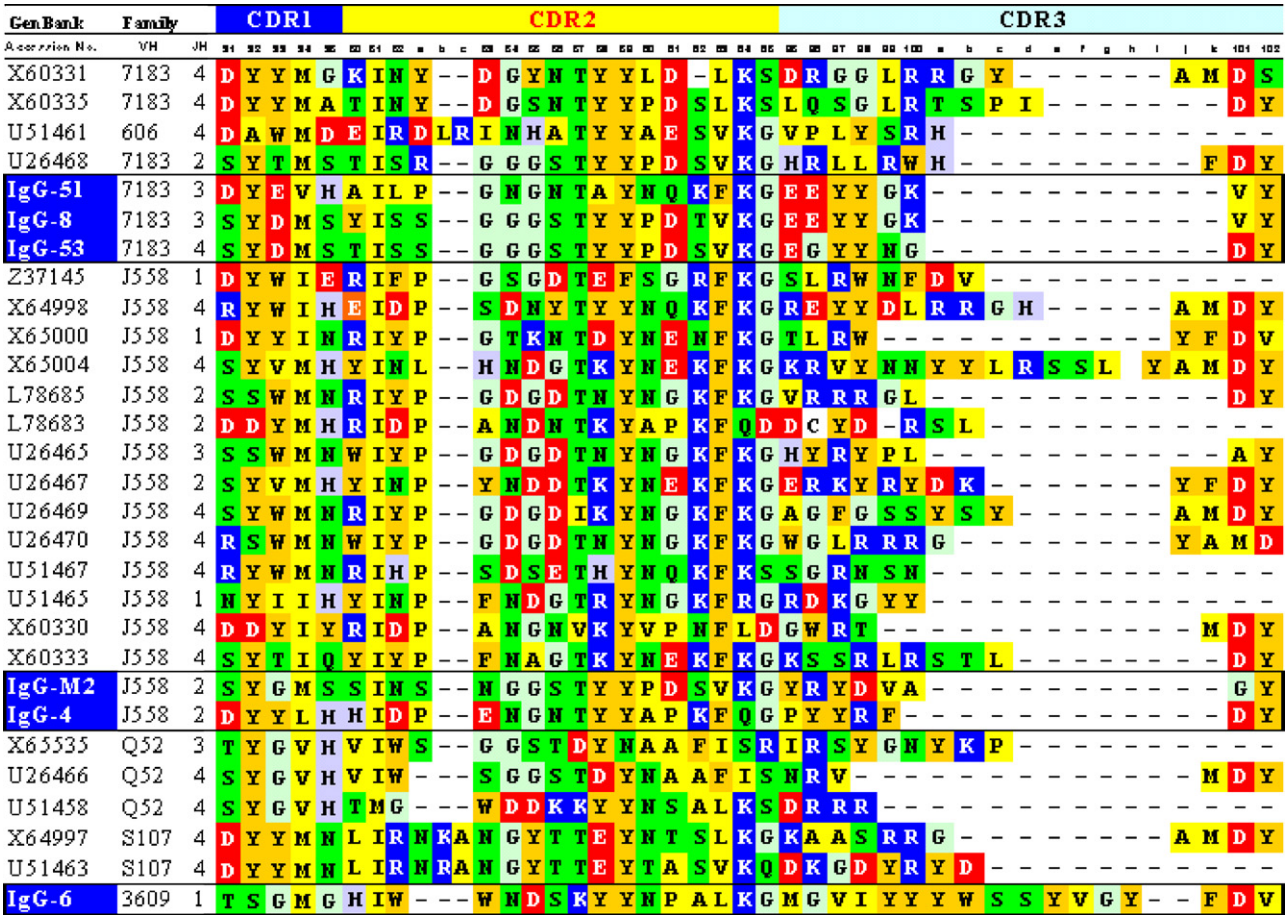

Fig. 2. Multialignment sequences of the amino acid residues in the CDR regions of CMV-specific Abs with anti-DNA Abs, the CDRs are indicated above the appropriate sequence segments in the table. Amino acids are identified by a single-letter code. A dash in the individual sequences denotes a deletion. The amino acid residues are numbering according to Kabat numbering [16].

Fig. 3. Alignments of anti-CMV light chain germline VκII, bd2 gene whose consensus amino acid sequences of V_L regions of the mAbs-specific CMV-CP belong to the Vκ2 gene bd2 (A) and Vκ1A gene bb1.1 gene (B) from the V_L regions GenBank database using IgBlast (Altschul et al. [20]; http://www.ncbi.nlm.nih.gov/igblast/). A dot in the individual sequences denotes amino acids that are the same as the consensus. The framework and complementarity-determining regions (CDRs) are indicated above the appropriate sequence segments in the figure. The amino acid residues are numbered according to Kabat numbering [16].

3.6. Molecular homology sequence of the V_L with GenBank database

The light chains of the CMV-specific Abs could be assigned to two major Vκ groups, Vκ2 or Vκ1A (Fig. 3), with sequence identity between the different light chains of each class ranging from 90 to 100% at the amino acid level. All 10 Abs use a V_L region encoded by Vκ 2-Jκ1 or -Jκ2 recombination; in addition, the Tyr residue was more frequently observed in 8 mAbs at the Vκ–Jκ joint (V_L96). This residue is encoded by Jκ2, while the Gln residue was observed twice at position V_L96 while the Trp residue was observed once at the same position, V_L96. Interestingly, the V_L34 residue is an Asn germline code VκII bd2 germline gene which is typical to Abs V_L-specific CMV-CP while the V_L-(4, 6, and 7), V_L34 Asn residue was substituted with Ser (Asn34Ser) (Fig. 3A). Moreover, the V_L gene was very restricted against CMV-CP, with high homology to numerous and different Abs raised against autoimmune diseases (anti-DNA, -RNA, -Sm, and -histone) as well as some human viruses (HIV-Gp41 and p24; Hepatitis B and C virus), and catAb proteolytic light chain, esterase-like catAb, and Ab catalysis of the cationic cyclization reaction (Fig. 3A). Four Abs used another VκIA-Jκ4 (Fig. 3B) which revealed high homology with the light chain against different specific antigens whose identity varied from 94 to 98% with light chains from the database i.e., influenza hemagglutinin neutralizing Ab, anti-ssDNA, -RNA, -fluorescein, -polysaccharide, and -bisphenol-A (Fig. 3B) suggesting an intrinsic polyspecificity associated with the V_L. In fact, Vκ1 is common to a relatively large population of Abs that bind a large number of antigens, including proteins, DNA, steroids, peptides, and small haptens [37]. Thus, the polyspecificity intrinsic to Vκ1 may contribute to the ability of the germline repertoire to bind to a wide array of chemical structures.

3.7. The relative activity of mAbs against pUC19 DNA

Indeed, there are numerous reports regarding natural catAbs but databases of the germline sequence are actually rare and the catalytic domain is mostly revealed from the V_L gene while the germline genes VκIA bb1.1 and VκII bd2 have been reported to possess DNase peptidase-like activity, respectively. Particularly, the Abs derived from germline gene VκII bd2 showed higher relative activity than that derived from germline gene VκIA bb1 (Fig. 4). Furthermore, the relative DNAse catalytic activity might depend on the V_H germline. In this case, in the presence of Mg^{2+}, most mAbs showed high DNA catalytic activity within a varying pH range (Fig. 4). Alternatively, the mAbs showed only a single break in linear DNA at pH 7–10 in the absence of Mg^{2+} (Fig. 4B, D, F, H, and L). In contrast, polyclonal antibodies (pAbs) illustrated a very restricted pH range, 7–7.5 (Fig. 4I and G). mAbs 5 and 6 revealed the disappearance of DNA in the presence of Mg^{2+} (Fig. 4C and E) while mAbs 4 and M2-4 showed less activity than mAb-5 and -6 (Fig. 4A and G). Notably, incubation of mAbs with CMV, polyglutamic acid, and dextrin sulphate efficiently inhibited DNase catalytic activity [15]. Remarkably, mAbs having different V_H combining ability with one V_L showed different DNase catalytic activity; therefore, we speculate that V_H could increase or decrease catalytic activity depending on the germline genes (Fig. 4 and Table 1).

3.8. Homology modeling of the 4-FV of IgG4 antibody

A three-dimensional structure of 4-FV is built by means of homology modeling for predicting the DNA catalytic mechanism. The V_L and V_H sequences of the IgG4 Ab share a very high level of identity with known Abs for which a crystal structure has been reported [38]. Superposition of homology modeled 4-FV structure

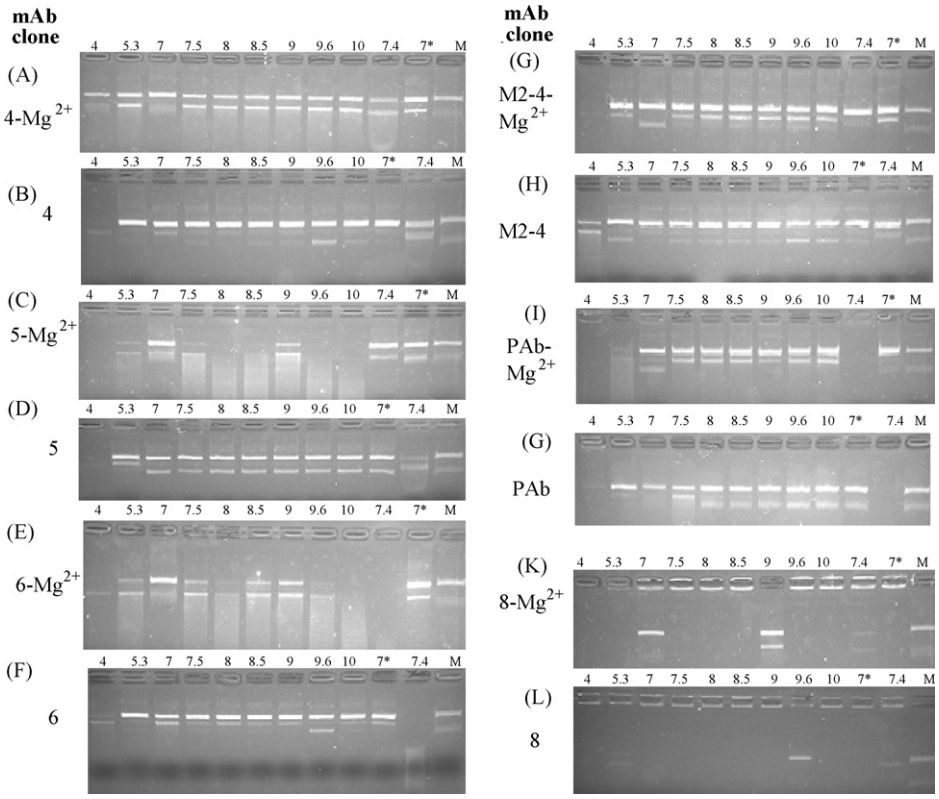

Fig. 4. The relative DNase activities of catalytic mAbs-specific CMV in cleavage of supercoild plasmid DNA pUC19. Variation in pH (4–10) conditions, lanes (4, 5.3) 50 mM NaOAc pH 4 and 5.3 buffer, respectively. Lane (7) 50 mM potassium phosphate buffer pH 7. Lanes (7.5, 8, 8.5, and 9) 50 mM Tris–HCl buffer pH 7.5, 8, 8.5, and 9, respectively. Lane (9.6) 50 mM carbonate buffer (pH 9.6). Lane (10), 50 mM borate buffer (pH 10). Lane (7.4) 20 mM Hepes buffer 10 mM NaCl, 1 mM $MgCl_2$, and 1 mM $MnCl_2$. Mg^{2+}: all buffers contain 5 mM Mg^{2+}. Lane (7*) 50 mM Tris–HCl free Mg^{2+}.

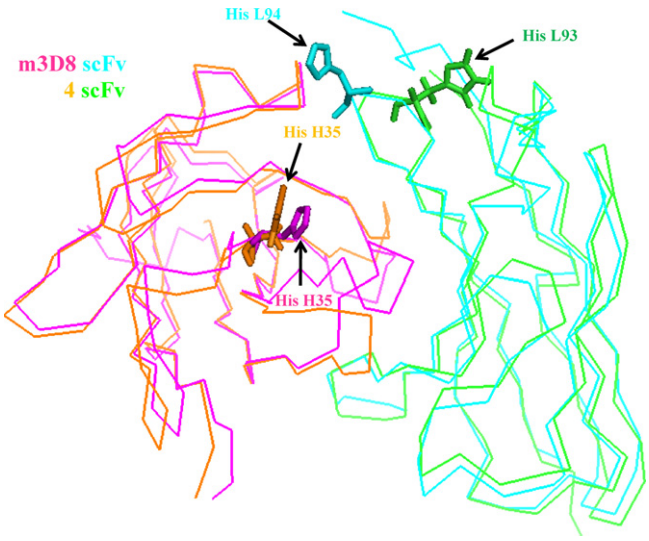

Fig. 5. Superposition of homology modeled 4-FV structure with the crystal structure of m3D8 scFv (PDB 2GKI) [38]. The alpha carbon traces of V_H and V_L domains of m3D8 and 4 are displayed in the indicated color code. Two critical residues for the catalysis (HisH35 and HisL93). The images were generated using PyMol software (DeLano Scientific LLC). (For interpretation of the references to color in this figure legend, the reader is referred to the web version of the article.)

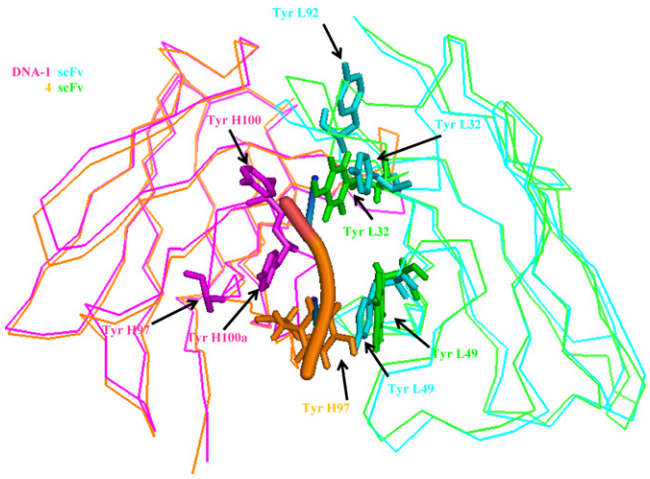

Fig. 7. Superposition of homology modeled 4-FV structure with the crystal structure DNA-1 anti-ssDNA Ab was drawn based on the X-ray structure of the DNA-1 Fab–dT3 complex and the molecular model of 4-FV. Superposition of the active sites of 4-FV with the active sites of anti-ssDNA (DNA-1) Abs indicates that Tyr L32, L49, Tyr L92 (turquoise), H97, H100 and H100a (pink) residues bind with dT3 (brown). The putative DNA binding residues of 4-FV with ssDNA are Tyr L32, L49 (green), and H97 (brown). The amino acid residues are represented by a three-letter code, and are numbered according to Kabat numbering (16). (For interpretation of the references to color in this figure legend, the reader is referred to the web version of the article.)

with the crystal structure of m3D8 scFv (PDB 2GKI) [38]. The alpha carbon traces of V_H and V_L domains of m3D8 and 4 are displayed in the indicated color code. Two critical residues for the catalysis (HisH35 and HisL93) with a similar orientation of key residues, potentially implied in the catalysis, were observed (Fig. 5) and putative DNA binding residues (Tyr residues at L32, L49, and H97) are highlighted as a stick model. The images were generated using PyMol software (DeLano Scientific LLC). The 3D structure similarity, added to the ability of 4-FV to hydrolyze DNA, suggest that the active sites of both catalysts probably have structural similarities. Superposition of the active sites of 4-FV to predict the binding site with the active sites of anti-DNA (m3D8) Ab indicates that Tyr [L32, L49 (green) and H97 (brown)] residues of 4-FV are equidistant to Tyr [L32, L49, L92 (turquoise), H97, and H100a (pink)] residues of the DNA catalytic m3D8 Ab (Fig. 6). Furthermore, superposition of the active sites of 4-FV with the active sites of anti-ssDNA (DNA-1) Abs indicates that Tyr [L32, L49, and L92 (turquoise)], Tyr [H97, H100 and H100a (pink)] residues binding with dT3 (brown) are at similar distances to Tyr [L32, L49 (green), and H97 (brown)] (Fig. 7). The structure shows that Ab binds oligo(dT) primarily by sandwiching thymine bases between Tyr side-chains, which allows the bases to make sequence-specific hydrogen bonds (Figs. 6 and 7). The 3D model is assessed by simulation of molecular dynamics to determine its stability and by comparison with those of known protein structures. The structural information from the theoretically modeled complex can help us to further understand the catalytic mechanism of anti-DNA Abs.

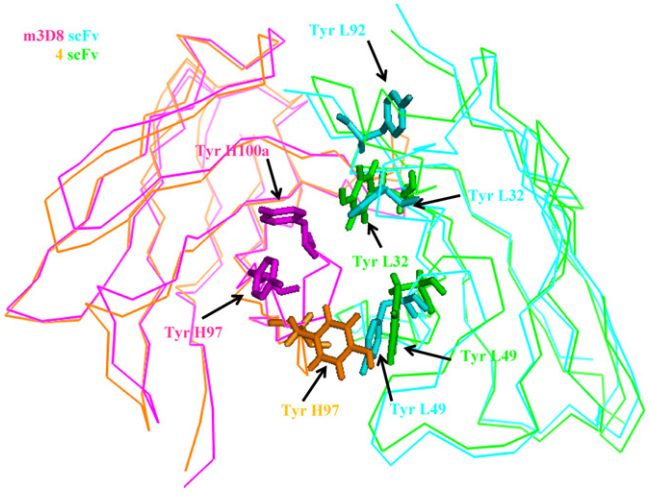

Fig. 6. Superposition of homology modeled 4-FV structure with the crystal structure of m3D8 scFv the putative DNA binding residues (Tyr residues at H97, L32, and L49) are highlighted as a stick model. The images were generated using PyMol software (DeLano Scientific LLC).

4. Discussion

Using data from known Ab crystal structures and computer modeling, a series of linkers were designed and evaluated as potential candidates to genetically connect the V_H and V_L regions. The resulting scFv molecules were evaluated for their functional activities and relative affinity [39]. Very little molecular characterization of natural catalytic Abs with mAbs has been achieved so far. Due to the activation of the immune system as a response to a foreign antigen, maturation of the Ab response takes place, resulting in the production of specific, high-affinity Abs. Therefore, specific Abs can be selected using a relatively small, random combinatorial V gene library derived from an immunized donor [40]. The procedure included the isolation of the V_H and V_L of the murine mAb from mRNA of 14 hybridoma cells, followed by cloning, sequencing and characterization of the FV. V_H gene usage was determined and compared to V_H genes used by Ab fragments of a germline database. The V_H and Vκ regions of 14 anti-CMV mAbs generated from five different fusions of BALB/c mice were immunized with native CMV-CP, and the V_H, D, J_H, Vκ, and Jκ were determined (Table 1). All the Abs were derived from distinct B cells because they had utilized diverse V_H, D, and J_H gene combinations, and because the length of the CDR3 region ranged from 7 to 17 amino acid residues (Table 2). An abundance of V_H genes from the J558 family was observed (8/14) but each represented a separate member of the family (Table 1). The V_L is encoded by the Vκ1 gene, which is common to a relatively large population of Abs that bind a large number of antigens including proteins, DNA, steroids, pep-

tides, and small haptens [37]. Certain combinations of germline V genes (Vκ, Jκ and V_H) are polyspecific in nature and can be used to construct Ab-combining sites for structurally very distinct ligands. Germline Ab polyspecificity further expands the binding potential of the germline repertoire [37]. This polyspecificity may be general to several germline-encoded Abs and may have been selected for by the immune system to provide a mechanism for rapid generation of Abs of moderate to high affinity for a broad range of antigens [37]. CMV-CP is capable of inducing a variety of B cells that have distinct phenotypic and genotypic paratopes. Interestingly, the high DNase catalytic Abs were encoded by germline genes such as mAb-8 (Fig. 1C). Furthermore, analysis of DNase catalytic activities and nucleotide sequences of the V_H and V_L showed a strong correlation with the germline heavy chains, in which mAb-(8) was derived from V_H7183, showing high DNase catalytic activity (Fig. 4K and L). Prominently, the result of the relative activity of the six different mAbs (4, 5, 6 and 8) showed diverse relative activities, although their light chain genes had high relative identity; therefore, the fact that V_H domain can modulate catalytic activity is potentially important in these mAbs (Fig. 4). One of the important aspects of V_L and V_H amino acid sequences is the study of the structural analysis of the antigen-binding loops by molecular modeling and simulation of molecular dynamics. Through these findings, amino acid His (H35 and L93) residues may play a crucial role in the DNA–Ab interaction (Fig. 5). Tyr (L32, L49 and H97) side-chains that exist in the antigen combining site might be capable of mediating most of the contacts necessary for DNA recognition, and thus it seems likely that the overabundance of Tyr in natural antigen-binding sites is a consequence of the side chain being particularly well suited for making productive contacts with antigen [41]. Interestingly, the genes encoding the heavy chain variable region of these Abs displayed evidence of only minimal somatic hypermutation (Fig. 1C). We consider that the negative charge on the acetate group in the CMV-CP was partially neutralized by a hydrogen bond with the phenolic hydroxyl group of tyrosine, which exists in HCDR3. Therefore, we speculate and expect that the HCDR3-peptide be used as tool for plant virus resistance depending on the peptide-neutralizing epitope.

5. Conclusion

We generated 14 mAbs raised by immunization with CMV that displayed DNase activity. Genes coding for V_H and V_L regions of all 14 mAbs were cloned and sequenced. The sequences were compared with sequences of the Ig-Blast database to determine their germline and to identify potential mutations responsible for DNA binding and DNase activity. Superposition of homology modeled 4-FV structure with the crystal structure of m3D8 scFv, two critical residues for catalysis (HisH35 and HisL93) and putative DNA binding residues (Tyr residues at L32, L49, and H97). Collectively our studies suggest that DNA binding and hydrolyzing activities of anti-CMV Abs are well conserved in both V_H and V_L, providing avenue to further studies of their biochemical and biological functions.

Acknowledgments

We are grateful to Professor Dr. Ikuo Fujii for his advice and helpful discussion. The authors would like to thank Dr. Yong-Sung Kim, Department of Genetic Engineering, Sungkyunkwan University Korea, for his grateful help in the antibody-docking.

References

[1] Pollack SJ, Jacobs JW, Schultz PG. Selective chemical catalysis by an antibody. Science 1986;234:1570–3.
[2] Tramontano A, Janda KD, Lerner RA. Catalytic antibodies. Science 1986;234:1566–70.
[3] Matsuura K, Ikoma S, Sugiyama M, Funauchi M, Sinohara H. Amidase and peptidase activities of polyclonal immunoglobulin G present in the sera of patients with rheumatoid arthritis. Appl Biochem Biotechnol 2000;83:107–13.
[4] Lacroix-Desmazes S, Moreau A, Sooryanarayana Bonnemain C, Stieltjes N, Pashov A, Sultan Y, et al. Catalytic activity of antibodies against factor VIII in patients with hemophilia A. Nat Med 1999;5:1044–7.
[5] Sinohara H, Matsuura K. Does catalytic activity of Bence–Jones proteins contribute to the pathogenesis of multiple myeloma? Appl Biochem Biotechnol 2000;83:85–94.
[6] Paul S, Kalaga RS, Gololobov G, Brenneman D. Natural catalytic immunity is not restricted to autoantigenic substrates: identification of a human immunodeficiency virus gp 120-cleaving antibody light chain. Appl Biochem Biotechnol 2000;83:71–84.
[7] Shuster AM, Gololobov GV, Kvashuk OA, Bogomolova AE, Smirnov IV, Gabibov AG. DNA hydrolyzing autoantibodies. Science 1992;256:665–7.
[8] Gao QS, Sun M, Tyutyulkova S, Webster D, Rees A, Tramontano A, et al. Molecular cloning of a proteolytic antibody light chain. J Biol Chem 1994;269:32389–93.
[9] Hifumi E, Mitsuda Y, Ohara K, Uda T. Targeted destruction of the HIV-1 coat protein gp41 by a catalytic antibody light chain. J Immunol Methods 2002;269:283–98.
[10] Rahman A, Latchman DS, Isenberg DA. Immunoglobulin variable region sequences of human monoclonal anti-DNA antibodies. Semin Arthritis Rheum 1998;28:141–54.
[11] Radic MZ, Weigert M. Genetic and structural evidence for antigen selection of anti-DNA antibodies. Annu Rev Immunol 1994;12:487–520.
[12] Nitta N, Masuta C, Kuwata S, Takanami Y. Comparative studies on the nucleotide sequence of Cucumber mosaic virus RNA3 between Y strain and Q strain. Ann Phytopathol Soc Japan 1988;54:516–22.
[13] Harlow E, Lane D. Antibodies. A laboratory manual. Cold Spring Harbor, NY: Cold Spring Harbor Laboratory Press; 1988.
[14] Huse WD, Sastry L, Iverson SA, Kang AS, Alting-Mees M, Burton DR, et al. Generation of a large combinatorial library of the immunoglobulin repertoire in phage lambda. Science 1989;246:1273–8.
[15] Zein HS, Teixeira da Silva JA, Miyatake K. Monoclonal antibodies specific to Cucumber mosaic virus coat protein possess DNA-hydrolyzing activity. Mol Immunol 2009;46:1527–33.
[16] Martin ACR. Accessing the Kabat antibody sequence database by computer PROTEINS: structure. Funct Genet 1996;25:130–3.
[17] Baker D, Sali A. Protein structure prediction and structural genomics. Science 2001;294:93–6.
[18] Paul S, Volle DJ, Beach CM, Johnson DR, Powell MJ, Massey RJ. Catalytic hydrolysis of vasoactive intestinal peptide by human autoantibody. Science 1989;244:1158–62.
[19] Nevinsky GA, Buneva VN. Natural catalytic antibodies—abzymes. In: Keinan E, editor. Catalytic antibodies. VCH–Wiley; 2004. p. 503–67.
[20] Altschul SF, Madden TL, Schaffer AA, Zhang J, Zhang Z, Miller W, et al. Gapped BLAST and PSI-BLAST: a new generation of protein database search programs. Nucl Acids Res 1997;25:3389–402.
[21] Schaeble KF, Thiebe R, Bensch A, Brensing-Kueppers J, Heim V, Kirschbaum T, et al. Characteristics of the immunoglobulin Vkappa genes, pseudogenes, relics and orphons in the mouse genome. Eur J Immunol 1999;29:2082–6.
[22] Cohen JB, Givol D. Allelic immunoglobulin VH genes in two mouse strains: possible germline gene recombination. EMBO J 1983;2:2013–8.
[23] Haines BB, Angeles CV, Parmelee AP, McLean PA, Brodeur PH. Germline diversity of the expressed BALB/c VhJ558 gene family. Mol Immunol 2001;38:9–18.
[24] Chang S, Mohan C. Identification of novel VH1/J558 immunoglobulin germline genes of C57BL/6 (Igh b) allotype. Mol Immunol 2005;11:1293–301.
[25] Gubbins MJ, Plummer FA, Yuan XY, Johnstone D, Drebot MA, Andonova M, et al. Molecular characterization of a panel of murine monoclonal antibodies specific for the SARS-coronavirus. Mol Immunol 2004;42:125–36.
[26] Chukwuocha RU, Hartman AB, Feeney AJ. Sequences of four new members of the VH7183 gene family in BALB/c mice. Immunogenetics 1994;40:76–8.
[27] Zhou YH, Sugitani M, Esumi M. Sequences in the hypervariable region 1 of hepatitis C virus show only minimal variability in the presence of antibodies against hypervariable region 1 during acute infection in chimpanzees. Arch Virol 2002;147:1955–62.
[28] Hoffmüller U, Knaute T, Hahn M, Höhne W, Schneider-Mergener J, Kramer A. Evolutionary transition pathways for changing peptide ligand specificity and structure. EMBO J 2000;19:4866–74.
[29] Calcutt MJ, Komissarov AA, Marchbank MT, Deutscher SL. Analysis of a nucleic-acid-binding antibody fragment: construction and characterization of heavy-chain complementarity-determining region switch variants. Gene 1996;168:9–14.
[30] Li J, Geissal ED, Li W, Stollar BD. Repertoire diversification in mice with an IgH-locus-targeted transgene for the rearranged VH domain of a physiologically selected anti-ssDNA antibody. Mol Immunol 2005;42:1475–84.
[31] Lee HA, Morgan MRA. Food immunoassays: applications of polyclonal, monoclonal and recombinant antibodies. Trends Food Sci Technol 1993;4:129–34.
[32] Castilla J, Sola I, Enjuanes L. Interference of coronavirus infection by expression of immunoglobulin G (IgG) or IgA virus-neutralizing antibodies. J Virol 1997;71:5251–8.
[33] Chen L, Chang S, Mohan C. Molecular signatures of antinuclear antibodies contributions of heavy chain CDR residues. Mol Immunol 2002;39:333–47.

[34] Diaw L, Magnac C, Pritsch O, Buckle M, Alzari PM, Dighiero G. Structural and affinity studies of IgM polyreactive natural autoantibodies. J Immunol 1997;158:968–76.
[35] Rini JM, Schulze-Gahmen U, Wilson IA. Structural evidence for induced fit as a mechanism for antibody–antigen recognition. Science 1992;255:959–65.
[36] Guddat LW, Shan L, Broomell C, Ramsland PA, Fan Z, Anchin JM, et al. The three-dimensional structure of a complex of a murine Fab (NC10, 14) with a potent sweetener (NC174): an illustration of structural diversity in antigen recognition by immunoglobulins. J Mol Biol 2000;302:853–72.
[37] Romesberg FE, Spiller B, Schultz PG, Stevens RC. Immunological origins of binding and catalysis in a Diels-Alderase antibody. Science 1998;279:1929–33.
[38] Kim YR, Kim JS, Lee SH, Lee WR, Sohn JN, Chung YC, et al. Heavy and light chain variable single domains of an anti-DNA binding antibody hydrolyze both double and single-stranded DNAs without sequence specificity. J Biol Chem 2006;28:15287–95.
[39] Wörn A, Plückthun A. Stability engineering of antibody single-chain Fv fragments. J Mol Biol 2001;305:989–1010.
[40] Clackson T, Hoogenboom HR, Griffiths AD, Winter G. Making antibody fragments using phage display libraries. Nature 1991;352:624–8.
[41] Glaser SM, Yelton DE, Huse WD. Antibody engineering by codon-based mutagenesis in a filamentous phage vector system. J Immunol 1992;149:3903–13.